

Perturbation of the O–U–O Angle in Uranyl by Coordination to a 12-Membered Macrocycle

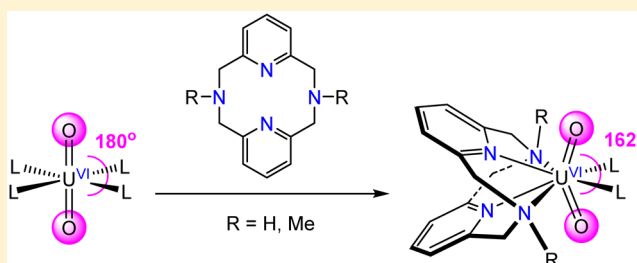
Elizabeth A. Pedrick,[†] Jason W. Schultz,[‡] Guang Wu,[†] Liviu M. Mirica,[‡] and Trevor W. Hayton^{*†}

[†]Department of Chemistry and Biochemistry, University of California Santa Barbara, Santa Barbara, California 93106, United States

[‡]Department of Chemistry, Washington University in St. Louis, St. Louis, Missouri 63130, United States

S Supporting Information

ABSTRACT: Reaction of $[\text{UO}_2\text{Cl}_2(\text{THF})_2]_2$ (THF = tetrahydrofuran) with 2 equiv of $^{\text{H}}\text{N}4$ ($^{\text{H}}\text{N}4$ = 2,11-diaza[3,3](2,6) pyridinophane) or $^{\text{Me}}\text{N}4$ ($^{\text{Me}}\text{N}4$ = *N,N'*-dimethyl-2,11-diaza[3,3](2,6) pyridinophane), in MeCN, results in the formation of $\text{UO}_2\text{Cl}_2(^{\text{R}}\text{N}4)$ (R = H; **1**; Me, **2**), which were isolated as yellow-orange solids in good yields. Similarly, reaction of $\text{UO}_2(\text{OTf})_2(\text{THF})_3$ with $^{\text{H}}\text{N}4$ in MeCN results in the formation of $\text{UO}_2(\text{OTf})_2(^{\text{H}}\text{N}4)$ (**3**), as an orange powder in 76% yield. Finally, reaction of $\text{UO}_2(\text{OTf})_2(\text{THF})_3$ with $^{\text{Me}}\text{N}4$ in THF results in the formation of $[\text{UO}_2(\text{OTf})(\text{THF})(^{\text{H}}\text{N}4)][\text{OTf}]$ (**4**), as an orange powder in 73% yield. Complexes **1–4** were fully characterized, including characterization by X-ray crystallography. These complexes exhibit the smallest O–U–O bond angles measured to date, ranging from $168.2(3)^\circ$ (for **2**) to $161.7(5)^\circ$ (for **4**), a consequence of an unfavorable steric interaction between the oxo ligands and the macrocycle backbone. A Raman spectroscopic study of **1–4** reveals no correlation between O–U–O angle and the $\text{U}=\text{O}$ ν_{sym} mode. However, complexes **1** and **2** do feature lower $\text{U}=\text{O}$ ν_{sym} modes than complexes **3** and **4**, which can be rationalized by the stronger donor strength of Cl^- versus OTf^- . This observation suggests that the identity of the equatorial ligands has a greater effect on the $\text{U}=\text{O}$ ν_{sym} frequency than does a change in O–U–O angle, at least when the changes in the O–U–O angles are small.



INTRODUCTION

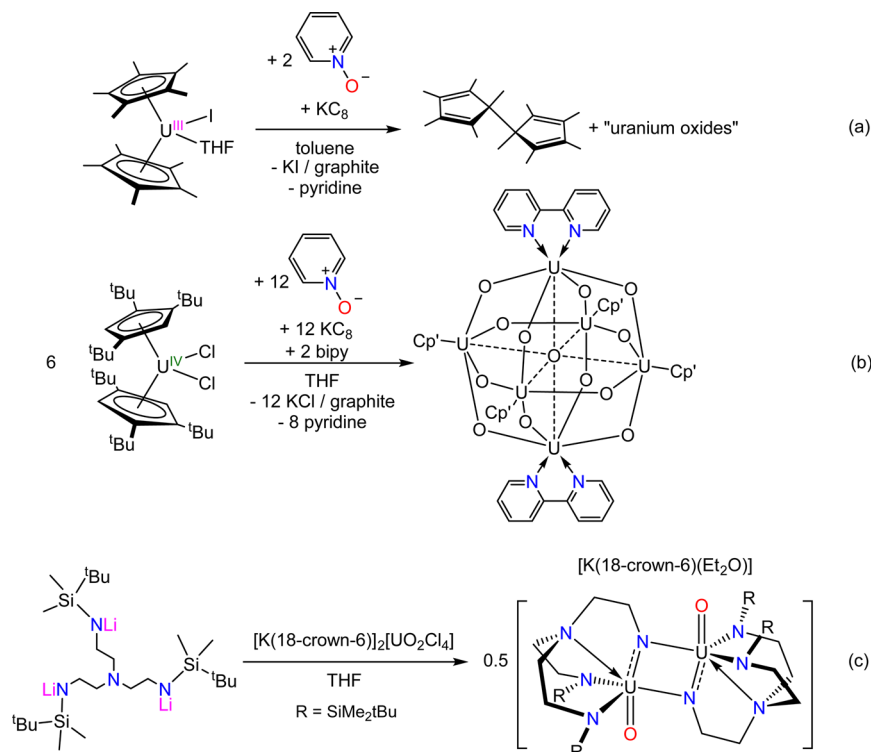
The uranyl ion, trans-UO_2^{2+} , is the most common fragment in uranium chemistry. It features short $\text{U}=\text{O}$ bond lengths (ca. 1.78 \AA)¹ and a trans arrangement of its two oxo ligands. Indeed, the O–U–O angle rarely deviates past 170° . This fixed stereochemistry has been rationalized by the presence of appreciable uranium $5f_z^3$ and $6p_z$ character within the O–U–O σ -bonding framework.^{1,2} In contrast to the ubiquity of the *trans*-uranyl fragment, the *cis*-uranyl ion is unknown, and all attempts to synthesize a *cis*-uranyl complex have been unsuccessful thus far.^{3–6} For example, reaction of $\text{Cp}^*_2\text{U}(\text{THF})$ (THF = tetrahydrofuran) with KC_8 and pyridine-*N*-oxide, in an attempt to generate *cis*- Cp^*_2UO_2 , resulted in formation of the pentamethylcyclopentadienyl dimer and “uranium oxides” (Scheme 1a).⁷ Similarly, reaction of $\text{Cp}'_2\text{UCl}_2$ ($\text{Cp}' = 1,2,4\text{-C}_3\text{H}_2\text{Bu}_3$) with pyridine-*N*-oxide and KC_8 afforded a mixed-valent uranium oxo cluster (Scheme 1b).⁸ Clark and co-workers attempted to enforce *cis*-oxo stereochemistry by ligating a tripodal ligand to the uranyl framework. However, reaction of $[\text{Li}]_3[\text{N}(\text{CH}_2\text{CH}_2\text{N-Si}^t\text{BuMe}_2)_3]$ with $[\text{K}(18\text{-crown-6})]_2[\text{UO}_2\text{Cl}_4]$ only resulted in formation of a mixed-valent U(V/VI) oxo-imido dimer, $[\text{K}(18\text{-crown-6})(\text{Et}_2\text{O})][\text{UO}(\mu_2\text{-NCH}_2\text{CH}_2\text{N}(\text{CH}_2\text{CH}_2\text{N-Si}^t\text{BuMe}_2)_2)]_2$ (Scheme 1c).³ In these three examples, the formation of the desired *cis*-oxo complex was thwarted by either ligand oxidation or ligand decomposition, which suggests that

the successful isolation of *cis*-uranyl will require the use of a robust, redox-inactive coligand.

While a *cis*-uranyl complex remains elusive, several *cis*-bis(imido) complexes are known, including *cis*- $\text{Cp}^*_2\text{U}(\text{NPh})_2$ and *cis*- $\text{Cp}_2\text{U}(\text{N}^t\text{Bu})_2$.^{4,9,10} Their higher stability, relative to the unobserved oxo analogue, is probably due to a greater reliance on π -bonding within the $[\text{U}(\text{NR})_2]^{2+}$ fragment, which diminishes the importance of the $6p$ orbital participation in the σ -bonding framework.¹¹ Similarly, Arnold and co-workers recently reported the isolation of $[\text{K}]_2[(\text{OUO})_2(\text{L})]$ (L = polypyrrole macrocycle), which is formally generated by coupling of a *trans*- $[\text{U}^{\text{V}}\text{O}_2]^+$ fragment with a *cis*- $[\text{U}^{\text{V}}\text{O}_2]^+$ fragment within the binding pocket of the polypyrrole macrocycle.^{12,13} In this case, reduction of both uranium ions to U(V) likely lowers the energy penalty required for *cis*/*trans* isomerization. In this regard, oxidation of this complex with pyridine-*N*-oxide results in rearrangement of the *cis*-di(oxo) fragment back to the original *trans* structure. Consistent with this result, density functional theory (DFT) studies of $[\text{UO}_2(\text{OH})_4]^{2-}$ reveal that the *cis* isomer is 18–20 kcal/mol higher in energy than the *trans* isomer, depending on the method used.^{14,15} Similarly, calculations reveal that the *cis* isomer of $[\text{UO}_2(\text{N}(\text{SiH}_3)_2)_3]^-$ is 31 kcal/mol less stable than

Received: March 30, 2016

Published: May 13, 2016

Scheme 1. Previous Attempts^a to Generate a *cis*-Uranyl Complex

^aReaction (a) taken from ref 7. Reaction (b) taken from ref 8. Reaction (c) taken from ref 3.

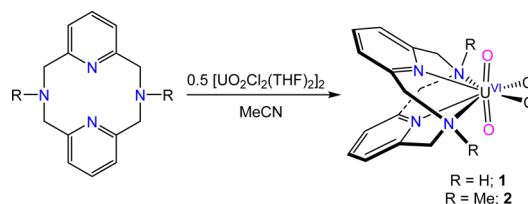
the *trans* isomer.¹⁶ These large destabilizations likely reflect the lack of an inverse trans influence (ITI) in the *cis*- UO_2^{2+} fragment^{17–21} and further highlight the challenges inherent in isolating a *cis*-uranyl complex. Despite these challenges, though, there is still considerable interest in the synthesis of an authentic *cis*-uranyl complex, as this fragment would provide unique insights into actinide covalency and f-orbital participation in bonding.¹

Drawing inspiration from the results of Clark and co-workers, we sought to coordinate a polydentate ligand, specifically a macrocyclic ligand, to the uranyl fragment to effect a *trans* to *cis* isomerization of the oxo ligands. Several researchers have previously explored the coordination of macrocycles to the uranyl ion. For example, Sessler and co-workers have demonstrated that the uranyl ion can fit within the binding pocket of the 20-membered pentaphyrin ligand.²² With this large binding pocket there is no steric pressure placed upon the two oxo ligands, and, as a result, the *trans* configuration is observed experimentally.^{22–24} In contrast, there are no known uranyl porphyrin complexes, likely because the uranyl ion cannot be accommodated by the binding pocket of the smaller 16-membered porphyrin core.²³ These observations suggest that coordination of uranyl to a small (≤ 16 -member ring size) macrocycle could effect the desired *trans/cis* isomerization. Accordingly, we sought to explore the reactivity of the uranyl ion with the 12-membered macrocyclic ligands, $^{\text{H}}\text{N4}$ ($^{\text{H}}\text{N4} = 2,11\text{-diaz}[3,3](2,6)$ pyridinophane) and $^{\text{Me}}\text{N4}$ ($^{\text{Me}}\text{N4} = N,N'\text{-dimethyl-}2,11\text{-diaz}[3,3](2,6)$ pyridinophane), which were shown recently to act as tetradentate ligands for transition metal ions, while leaving two open coordination sites in a *cis* arrangement.^{25–27}

RESULTS AND DISCUSSION

Addition of 2 equiv of $^{\text{H}}\text{N4}$ to $[\text{UO}_2\text{Cl}_2(\text{THF})_2]_2$ in MeCN, results in the formation of a yellow-orange slurry, from which $\text{UO}_2\text{Cl}_2(^{\text{H}}\text{N4})$ (**1**) can be isolated as a yellow crystalline solid in 66% yield (Scheme 2). Similarly, addition of 2 equiv of $^{\text{Me}}\text{N4}$ to

Scheme 2. Synthesis of Complexes 1 and 2



$[\text{UO}_2\text{Cl}_2(\text{THF})_2]_2$ in MeCN, results in the formation of an orange-yellow slurry, from which $\text{UO}_2\text{Cl}_2(^{\text{Me}}\text{N4})$ (**2**) can be isolated as a yellow-orange powder in 73% yield (Scheme 2).

Complex **1** crystallizes in the monoclinic space group $P2_1/m$ as the MeCN solvate, $1 \cdot 2\text{MeCN}$ (Figure 1), while complex **2** crystallizes in the orthorhombic space group $Cmcm$ as the MeCN solvate, $2 \cdot 2\text{MeCN}$ (Figure 1). Complex **2** is also isolable in a second crystal modification (**2a**), which occupies the orthorhombic space group $Pbcn$ (see Supporting Information). Both **1** and **2** feature eight-coordinate geometries, with all four nitrogen atoms of the macrocyclic ligand coordinating to the U centers. The O–U–O angles in **1** and **2** are $164.1(3)^\circ$ and $168.2(3)^\circ$, respectively (Table 1). These O–U–O angles are among the smallest reported for the uranyl fragment and are comparable to those observed for $\text{Cp}^*\text{UO}_2(^t\text{Bu-Mes-PDI}^{\text{Me}})$ (O–U–O = $167.4(4)^\circ$),²⁸ $[\text{NET}_4]_2[\text{UO}_2(\eta^5\text{-Cp}^*)(\text{CN})_3]$ (O–U–O = $168.40(9)^\circ$),²⁹

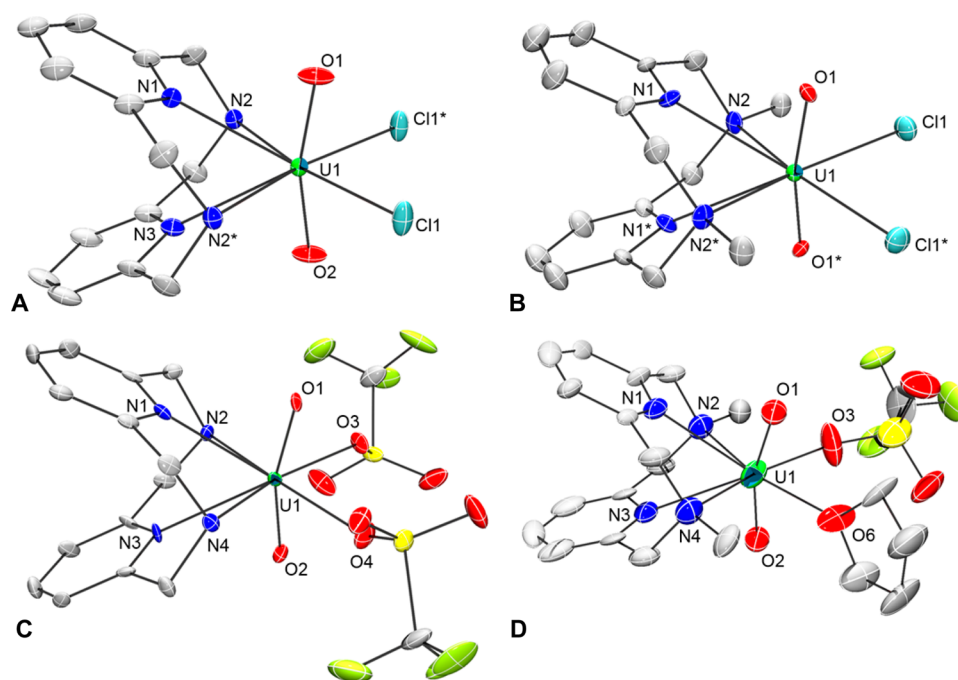


Figure 1. Solid-state structures of 1–4, with 50% probability ellipsoids. (A) Solid-state structure of $\text{UO}_2\text{Cl}_2(\text{H}^4\text{N}_4)\cdot 2\text{MeCN}$ (1·2MeCN). (B) Solid-state structure of $\text{UO}_2\text{Cl}_2(\text{Me}^4\text{N}_4)\cdot 2\text{MeCN}$ (2·2MeCN). (C) Solid-state structure of $\text{UO}_2(\text{OTf})_2(\text{H}^4\text{N}_4)$ (3). (D) Solid-state structure of $[\text{UO}_2(\text{OTf})(\text{THF})(\text{Me}^4\text{N}_4)][\text{OTf}]\cdot 0.5\text{C}_4\text{H}_8\text{O}$ (4·0.5C₄H₈O). Counterions, solvate molecules, and all hydrogen atoms were omitted for clarity.

Table 1. Selected Bond Lengths (Å) and Angles (deg) for Complexes 1–4

| | 1 | 2 | 2a | 3 | 4 |
|-----------------------------------------------------------------|------------|------------|------------|------------|------------|
| U=O | 1.776(5) | 1.779(6) | 1.769(4) | 1.759(6) | 1.76(1) |
| U–N _{pyr} | 1.785(5) | 2.732(5) | 2.693(5) | 1.781(6) | 1.77(1) |
| | 2.639(6) | | | 2.626(7) | 2.68(1) |
| | 2.674(7) | | | 2.635(7) | 2.73(1) |
| U–N _R | 2.601(5) | 2.727(6) | 2.728(5) | 2.580(7) | 2.63(1) |
| U–Cl | | | | 2.597(7) | 2.67(1) |
| U–O _{OTf} | 2.735(1) | 2.686(2) | 2.677(2) | | |
| | | | | 2.397(6) | 2.34(1) |
| | | | | 2.409(6) | |
| O–U–O | 164.1(3) | 168.2(3) | 168.3(3) | 162.8(3) | 161.7(5) |
| N _{pyr} –U–N _{pyr} | 58.5(2) | 56.2(2) | 57.3(2) | 59.4(2) | 57.8(3) |
| distance of the N _{pyr} atom from the equatorial plane | av 1.298 Å | 1.288(5) Å | 1.083(5) Å | av 1.302 Å | av 1.305 Å |

$\text{UO}_2(\text{SCS})(\text{py})_2$ (SCS = C(PPh₂S)₂; O–U–O 168.5(1)°),³⁰ $[\text{UO}_2(\text{BIPM}^{\text{TMS}})(\text{DMAP})_2]$ (BIPM^{TMS} = C(PPh₂NSiMe₃)₂; DMAP = 4-(dimethylamino)pyridine; O–U–O = 167.16(9)°),³¹ $[\text{UO}_2(\text{O}-2,6\text{-}^t\text{Bu}_2\text{C}_6\text{H}_3)_2(\text{THF})_2]$ (O–U–O = 167.8(4)°),³² and $[\text{UO}_2(\kappa^2\text{-NO}_3)_2(\text{Prbtp})]$ (Prbtp = 2,6-bis(5,6-di-*n*-propyl-1,2,4-triazin-3-yl)pyridine; O–U–O = 166.2(1)°).³³ We suggest that the deviation from linearity in complexes 1 and 2, in particular, is due to an unfavorable steric interaction between the oxo ligands and the macrocycle backbone. In this regard, the smaller O–U–O angle in 1 versus 2 may be due to the shorter U–N_R (R = H, Me) and U–N_{pyr} bond lengths in the former, which is a result of the smaller steric profile of H⁴N₄ versus Me⁴N₄. A difference in M–N_R bond distances between H⁴N₄ and Me⁴N₄ can also be seen in $[\text{FeCl}_2(\text{H}^4\text{N}_4)][\text{Cl}]$ (Fe–N = 2.189(1) Å)³⁴ and $[\text{FeCl}_2(\text{Me}^4\text{N}_4)][\text{FeCl}_4]$ (Fe–N = 2.237(2) and 2.219(2) Å).³⁵ The U–O bond lengths in 1 (1.776(5) and 1.785(5) Å) and 2 (1.779(6) Å), in contrast to the O–U–O angles, are similar to those exhibited by *trans*-uranyl.³³ Interestingly, the N_{pyr}–M–N_{pyr} angles in 1 (58.5(2)°) and 2 (56.2(2)°) are much smaller

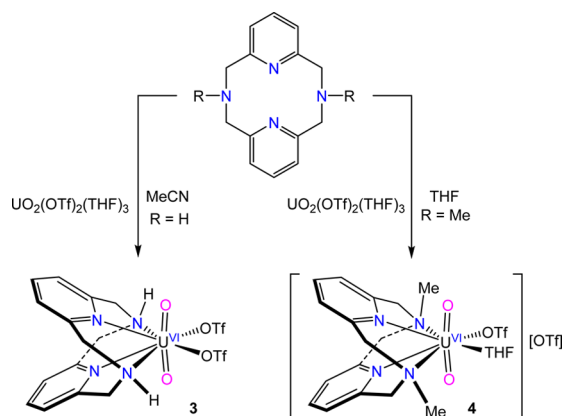
than those observed in other H⁴N₄ and Me⁴N₄ complexes,^{36–38} such as $[\text{Fe}(\text{H}^4\text{N}_4)\text{Cl}_2][\text{Cl}]$ (84.95(7)°),³⁴ $[\text{FeCl}_2(\text{Me}^4\text{N}_4)]\text{-}[\text{FeCl}_4]$ (78.05(8)°),³⁵ $\text{OsCl}_2(\text{Me}^4\text{N}_4)$ (82.4(3)°),³⁹ and $\text{MnCl}_2(\text{Me}^4\text{N}_4)$ (73.5(1)°).⁴⁰ This difference can be rationalized by greater steric constraints placed upon the R⁴N₄ ligands by the uranyl fragment in complexes 1 and 2.

Another interesting aspect of these structures is the displacement of the N atoms of the two R⁴N₄ pyridine rings from the uranyl equatorial plane (defined by U1, N2, N2*, Cl1, and Cl1* in 1 and U1, N2, and N2* in 2). In particular, the N_{pyr} atoms are displaced from the uranyl equatorial plane by 1.298 Å and 1.288(5) Å in 1 and 2, respectively (Table 1). Deviations of multiple donor atoms from the equatorial plane of the UO_2^{2+} ion are very rare, and only a handful of examples are known.^{33,41–45} For instance, the nitrogen atoms in $[\text{UO}_2(\text{terpy})_2][\text{OTf}]_2$ (terpy = 2,6-bis(2-pyridyl)pyridine) and $[\text{UO}_2(\text{phen})_3][\text{OTf}]_2$ (phen = 1,10-phenanthroline), feature maximum displacements from the uranyl equatorial plane of 0.49 and 0.71 Å, respectively.^{43,46} Similarly, an N atom in the recently reported $\text{UO}_2\text{Cl}_2(\text{H}_2\text{BBP})$ (H₂BBP = 2,6-bis(2-

benzimidazolyl)pyridine) is displaced from the uranyl equatorial plane by 0.74 Å.⁴¹ The most striking example of donor atom displacement from the equatorial plane is that exhibited by $[\text{NEt}_4]_2[\text{UO}_2(\eta^5\text{-Cp}^*)(\text{CN})_3]$. In this example, the maximum displacement of one of the carbon atoms on the cyclopentadienyl ring is 1.494(6) Å.²⁹

In an effort to strengthen (and shorten) the U–N bonds, and thereby decrease the O–U–O angle even further, we explored the substitution of the chloride ligands in **1** and **2** with weaker electron-donating pseudohalide ligands. Thus, addition of 1 equiv of ^HN4 to $\text{UO}_2(\text{OTf})_2(\text{THF})_3$ in MeCN results in formation of an orange solution, from which $\text{UO}_2(\text{OTf})_2(\text{H}^{\text{N4}})$ (**3**) can be isolated in a 76% yield as an orange powder (Scheme 3). Similarly, addition of 1 equiv of ^{Me}N4 to

Scheme 3. Synthesis of Complexes **3** and **4**



$\text{UO}_2(\text{OTf})_2(\text{THF})_3$ in THF results in formation of $[\text{UO}_2(\text{OTf})(\text{THF})(\text{Me}^{\text{N4}})][\text{OTf}]$ (**4**), which can be isolated as an orange powder in a 73% yield (Scheme 3). We also attempted the reaction of ^{Me}N4 and $\text{UO}_2(\text{OTf})_2(\text{THF})_3$ in MeCN. However, X-ray quality crystals could not be grown from this solvent.

Complex **3** crystallizes in the orthorhombic space group $Pna2_1$, while complex **4** crystallizes in the triclinic space group $P\bar{1}$ as a THF solvate, $4 \cdot 0.5\text{C}_4\text{H}_8\text{O}$ (Figure 1). As with complexes **1** and **2**, all four nitrogen atoms of the macrocyclic ligand are coordinated to the U centers in **3** and **4**. Complex **3** also features two $[\text{OTf}]^-$ ligands within its inner coordination sphere, while complex **4** features a THF ligand and an $[\text{OTf}]^-$ ligand within its inner coordination sphere. Gratifyingly, the O–U–O bond angles in **3** (162.8(3)°) and **4** (161.7(5)°) are smaller than those observed in **1** and **2** (Table 1) and, more significantly, are smaller than any O–U–O angles reported previously.^{29–33} These smaller angles are likely due to the exchange of chloride for the poorly electron donating $[\text{OTf}]^-$ ligands, which strengthens the U–N interactions. That said, the U–N_R and U–N_{pyr} distances in **3** and **4** are not significantly shorter than those observed in **1** and **2**. Similar to **1** and **2**, both complexes exhibit U=O distances that are typical of the uranyl fragment (**3**: 1.759(6) and 1.781(6) Å, **4**: 1.76(1) and 1.77(1) Å).⁴⁷ The other metrical parameters in **3** and **4**, including the N_{pyr}–U–N_{pyr} angles, are comparable to those observed in **1** and **2**.

In an effort to better understand the effect of coordinating the ^RN4 macrocycles to the uranyl fragment we turned to Raman spectroscopy. This technique has proven to be useful for probing the relative strengths of the U=O bond in the

uranyl fragment.⁴⁸ Raman spectroscopic data for complexes **1**–**4** are shown in Table 2. Complexes **1** and **2** exhibit $\text{U}=\text{O} \nu_{\text{sym}}$

Table 2. Comparison of the $\text{U}=\text{O} \nu_{\text{sym}}$ Stretching Frequency for a Series of Uranyl Complexes

| complex | $\text{U}=\text{O} \nu_{\text{sym, stretch}}$ (cm^{-1}) | ref |
|--------------------------------------------------------------------------------------------------------------------------------------------------------------|-----------------------------------------------------------------------|--------------|
| $[\text{UO}_2(\text{OH})_4]^{2-}$ | 784 | 51 |
| $\text{Cp}^*\text{UO}_2(\text{tBu}^{\text{Mes}}\text{PDI}^{\text{Me}})$ | 789 | 28 |
| $\text{UO}_2(\text{OAr})_2(\text{THF})_2$ (Ar = 2,6-Ph ₂ C ₆ H ₃) | 808 | 48 |
| $[\text{UO}_2(\text{CO}_3)_3]^{4-}$ | 812 | 49 |
| $\text{UO}_2(\text{Ar}^{\text{acnac}})_2$ (Ar ^{acnac} = ArNC(Ph)CHC(Ph)O; Ar = 3,5- ^t Bu ₂ C ₆ H ₃) | 812 | 50 |
| $\text{UO}_2\text{Cl}_2(\text{H}^{\text{N4}})$ (1) | 813 | ^a |
| $\text{UO}_2\text{Cl}_2(\text{Me}^{\text{N4}})$ (2) | 815 | ^a |
| $\text{UO}_2(\text{tBu}^{\text{acnac}})_2(\text{THF})$ (tBu ^{acnac} = ^t BuNC(Ph) CHC(Ph)O) | 823 | 50 |
| $\text{UO}_2(\text{dbm})_2(\text{THF})$ (dbm = OC(Ph)CHC(Ph)O) | 823 | 21 |
| $[\text{UO}_2(\text{OTf})(\text{THF})(\text{Me}^{\text{N4}})][\text{OTf}]$ (4) | 831 | ^a |
| $\text{UO}_2(\text{OTf})_2(\text{H}^{\text{N4}})$ (3) | 833 | ^a |
| $[\text{UO}_2\text{Cl}_2(\text{THF})_2]_2$ | 835 | ^a |
| $[\text{UO}_2(\text{Ph}_3\text{PO})_4][\text{OTf}]$ | 839 | 52 |
| $\text{UO}_2(\text{OTf})_2(\text{THF})_3$ | 842 | ^a |
| $[\text{UO}_2(\text{OAc})_3]^-$ | 843 | 49 |
| $[\text{UO}_2(\text{dppmo})_2\text{OTf}][\text{OTf}]$ (dppmo = Ph ₂ P(O) CH ₂ P(O)Ph ₂) | 849 | 53 |
| $[\text{UO}_2\text{Cl}_4]^{2-}$ | 854 | 49 |
| $[\text{UO}_2(\text{H}_2\text{O})_5]^{2+}$ | 870 | 49 |

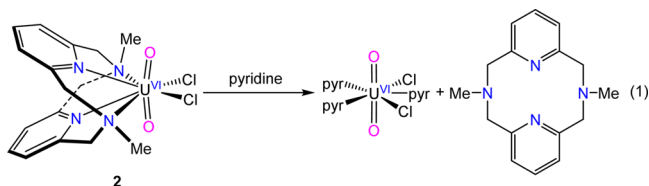
^aThis work.

modes at 813 and 815 cm^{-1} , respectively, in their Raman spectra. Interestingly, these values are on the lower end of the $\text{U}=\text{O} \nu_{\text{sym}}$ modes measured previously for the uranyl ion and are similar to those observed for uranyl complexes with anionic, electron-rich ligands, such as $[\text{UO}_2(\text{CO}_3)_3]^{4-}$ and $\text{UO}_2(\text{Ar}^{\text{acnac}})_2$ (Ar^{acnac} = ArNC(Ph)CHC(Ph)O; Ar = 3,5-^tBu₂C₆H₃).^{49,50} For further comparison, the $\text{U}=\text{O} \nu_{\text{sym}}$ mode in $[\text{UO}_2\text{Cl}_2(\text{THF})_2]_2$ was found to be 20 cm^{-1} higher, at 835 cm^{-1} . Both of these observations suggest that coordination of the macrocycle ligand to the uranyl ion does weaken the U–O bond to some extent. Complexes **3** and **4** exhibit $\text{U}=\text{O} \nu_{\text{sym}}$ modes at 833 and 831 cm^{-1} , respectively (Table 2), in their Raman spectra. For comparison, the $\text{U}=\text{O} \nu_{\text{sym}}$ mode in $\text{UO}_2(\text{OTf})_2(\text{THF})_3$ is observed at 842 cm^{-1} , an increase of ca. 10 cm^{-1} versus the values observed for **3** and **4**. Again, this difference can be interpreted as evidence that the U=O bonds in the uranyl moiety are weakened upon coordination of the ^RN4 macrocycle. That said, it is unlikely that the decrease in the $\text{U}=\text{O} \nu_{\text{sym}}$ mode observed upon coordination of ^RN4 to $[\text{UO}_2\text{Cl}_2(\text{THF})_2]_2$ or $\text{UO}_2(\text{OTf})_2(\text{THF})_3$ is due to the bending of the O–U–O fragment. Instead, this decrease is probably due to coordination of a relatively good tetradentate donor to the uranyl moiety. In addition, complexes **1** and **2**, despite featuring larger O–U–O angles than **3** and **4**, actually exhibit weaker U=O bonds (as indicated by their lower $\text{U}=\text{O} \nu_{\text{sym}}$ modes). Their weaker U=O bonds can be rationalized by the stronger donor strength of Cl[−] versus OTf[−], highlighting the fact that the identity of the equatorial ligands has a greater effect on the $\text{U}=\text{O} \nu_{\text{sym}}$ frequency than does a change in O–U–O angle, at least when the changes in the O–U–O angles are small.

Finally, we explored the chemical properties and solution-phase behavior of complexes **1**–**4**. Complexes **1**–**3** are insoluble in nonpolar, aromatic, and etheral solvents, and

only sparingly soluble in CH_2Cl_2 and MeCN. In contrast, complex **4** is somewhat soluble in THF and very soluble in CH_2Cl_2 and MeCN. The ^1H NMR spectrum of **1** in CD_2Cl_2 features diastereotopic methylene environments at 5.23 and 4.82 ppm for the $^{\text{H}}\text{N4}$ ligand, consistent with its ligation to a metal center (Figure S9).^{54–56} Similarly, the ^1H NMR spectrum of **2** in CD_2Cl_2 exhibits diastereotopic methylene resonances at 4.85 and 4.29 ppm for the $^{\text{Me}}\text{N4}$ ligand (Figure S11). Also observed in this spectrum is a singlet at 3.57 ppm, which is assignable to the two methyl substituents. The ^1H NMR spectrum of **3** in CD_2Cl_2 features diastereotopic methylene environments at 5.19 and 4.91 ppm for the $^{\text{H}}\text{N4}$ ligand (Figure S13).⁵⁴ In addition, this spectrum also features a broad resonance at 5.76 ppm, which we assigned to the NH substituent. The $^{19}\text{F}\{^1\text{H}\}$ NMR spectrum of **3** exhibits a singlet at -77.41 ppm. As observed for **3**, the ^1H NMR spectrum of **4** in CD_2Cl_2 exhibits diastereotopic methylene resonances at 4.87 and 4.53 ppm (Figure S17). The spectrum also features a CH_3 resonance at 3.59 ppm and two broad singlets at 3.73 and 1.84 ppm, which are assignable to the THF ligand. The $^{19}\text{F}\{^1\text{H}\}$ NMR spectrum of **4** in CD_2Cl_2 only exhibits a single resonance at -77.56 ppm, suggesting that the inner- and outer-sphere $[\text{OTf}]^-$ moieties undergo rapid exchange in solution.

Complexes **1–4** are also quite soluble in pyridine. However, dissolution of complex **2** in pyridine- d_5 results in displacement of the macrocycle from the uranyl coordination sphere, according to ^1H NMR spectroscopy, along with probable formation of $\text{UO}_2(\text{pyr})_3(\text{Cl})_2$ (eq 1).⁵⁷ This observation is



significant because it suggests that uranyl–macrocycle interaction in **2** is relatively weak; no doubt because of the mismatch between the uranyl ion and the $^{\text{Me}}\text{N4}$ macrocycle binding pocket. Dissolution of **1**, **3**, or **4** in pyridine does not result in macrocycle dissociation, likely because of the smaller steric profile of $^{\text{H}}\text{N4}$ (in the case of **1** and **3**) or the positive charge of the complex (in the case of **4**). Both effects are anticipated to strengthen the uranyl–macrocycle bonds.

CONCLUSION

Ligation of the 12-membered macrocyclic ligands $^{\text{H}}\text{N4}$ and $^{\text{Me}}\text{N4}$ to the uranyl ion results in the formation of the eight-coordinate complexes $\text{UO}_2\text{Cl}_2(\text{RN4})$ ($\text{R} = \text{H}$; **1**; Me, **2**), $\text{UO}_2(\text{OTf})_2(\text{H}^{\text{N4}})$ (**3**), and $[\text{UO}_2(\text{OTf})(\text{THF})(\text{Me}^{\text{N4}})] [\text{OTf}]^-$ (**4**). All four complexes feature O–U–O angles that are 168° or smaller. Complexes **3** and **4**, in particular, exhibit the smallest O–U–O angles yet reported. These small O–U–O angles are a result of steric repulsion between the oxo ligands of the uranyl fragment and the macrocycle backbone, which is a consequence of the small binding pocket of the $^{\text{R}}\text{N4}$ ligand. These results reveal that coordination of a small macrocycle to the uranyl ion is a viable strategy for the perturbation of the O–U–O angle. While coordination of $^{\text{H}}\text{N4}$ and $^{\text{Me}}\text{N4}$ to the uranyl ion did not result in trans/cis isomerization, as intended, our results do give some insight into new strategies for the generation of a cis-uranyl complex. For one, the relatively small $\text{N}_{\text{pyr}}\text{–U–N}_{\text{pyr}}$ angles extant in complexes **1–4** reveal that the

$^{\text{R}}\text{N4}$ macrocycles still feature significant flexibility. As a result, we suggest that future studies focus on macrocycles with even greater rigidity, such as the “cross-bridged” cyclam ligands.^{58,59}

Second, the coordination of an anionic macrocyclic ligand to uranyl, which would result in even shorter uranyl–macrocycle bonds on account of the greater electrostatic attraction to UO_2^{2+} , should also better promote the desired trans/cis isomerization.

EXPERIMENTAL SECTION

General. All reactions and subsequent manipulations were performed under anaerobic and anhydrous conditions under an atmosphere of nitrogen. Et_2O , THF, and toluene were dried by passage over activated molecular sieves using a Vacuum Atmospheres solvent purification system. CH_2Cl_2 , CD_2Cl_2 , MeCN, MeCN- d_3 , and pyr- d_5 were dried over activated 3 Å molecular sieves for 24 h before use. $[\text{UO}_2\text{Cl}_2(\text{THF})_2]$,⁴⁷ $\text{UO}_2(\text{OTf})_2(\text{THF})_3$,⁶⁰ $^{\text{H}}\text{N4}$,⁶¹ and $^{\text{Me}}\text{N4}$ ⁶² were prepared according to literature procedures. All other reagents were purchased from commercial suppliers and used as received.

NMR spectra were recorded on a Varian UNITY INOVA 400 spectrometer or a Varian UNITY INOVA 500 spectrometer. ^1H NMR spectra were referenced to external SiMe_4 using the residual protio solvent peaks as internal standards. The chemical shifts of $^{19}\text{F}\{^1\text{H}\}$ were referenced indirectly with the ^1H resonance of SiMe_4 at 0 ppm, according to IUPAC standard.^{63,64} IR spectra were recorded on a Mattson Genesis FTIR/Raman spectrometer. UV–vis–NIR experiments were performed on a UV-3600 Shimadzu spectrophotometer. Elemental analyses were performed by the Microanalytical Laboratory at UC Berkeley.

Raman Spectroscopy. Raman spectra were recorded on a LabRam Aramis microRaman system (Horiba Jobin Yvon), equipped with 1200 grooves/mm holographic gratings, and Peltier-cooled CCD camera. The 633 nm output of a Melles Griot He–Ne laser was used to excite the sample, and spectra were collected in a back-scattering geometry using a confocal Raman Microscope (high stability BX40) equipped with Olympus objectives (MPlan 50X). Sample preparation was performed inside the glovebox: Pure crystalline solid samples were placed between a glass microscope slide and coverslip, sealed with a bead of silicone grease, and removed from the glovebox for spectral acquisition.

X-ray Crystallography. The solid-state molecular structures of complexes **1–4** were determined similarly with exceptions noted in the following paragraph. Crystals were mounted on a cryoloop under mineral oil. Data collection was performed on a Bruker KAPPA APEX II diffractometer equipped with an APEX II CCD detector using a TRIUMPH monochromator with a Mo $K\alpha$ X-ray source ($\alpha = 0.71073$ Å). Data for **1–4** were collected at 100(2) K, using an Oxford nitrogen gas cryostream system. A hemisphere of data was collected using ω scans with 0.5° frame widths. Frame exposures of 5, 10, 15, 5, and 45 s were used for complexes **1**, **2**, **2a**, **3**, and **4**, respectively. Data collection and cell parameter determination were conducted using the SMART program.⁶⁵ Integration of the data frames and final cell parameter refinement were performed using SAINT software.⁶⁶ Absorption correction of the data was performed using the multiscan method SADABS.⁶⁷ Subsequent calculations were performed using SHELXTL.⁶⁸ Structure determination was done using direct or Patterson methods and difference Fourier techniques. All hydrogen atom positions were idealized and rode on the atom of attachment. However, hydrogen atoms were not assigned to the disordered carbon atoms. Structure solution, refinement, graphics, and creation of publication materials were performed using SHELXTL.⁶⁸

Complex **1** contains a MeCN solvent molecule that exhibits mild positional disorder about the methyl carbon atom. The positional disorder was addressed by modeling the CH_3 group in two orientations in a 50:50 ratio. Hydrogen atoms were not assigned to this carbon atom. Complex **1** was also mildly twinned. The twinning was subsequently revealed by using the program CELL_NOW.⁶⁹ Complex **2** contains two oxo ligands and two chloride ligands in the

Table 3. X-ray Crystallographic Information for 1–4

| | 1 | 2 | 2a |
|--------------------------------------------------------------|----------------------------------------------------------------------------------------------|------------------------------------------------------------------------------------------------|--------------------------------------------------------------------------------|
| empirical formula | UCl ₂ N ₆ O ₂ C ₁₈ H ₂₂ | UCl ₂ N ₆ O ₂ C ₂₀ H ₂₆ | UCl ₂ N ₄ O ₂ C ₁₆ H ₂₀ |
| crystal habit, color | block, yellow orange | shard, light yellow | block, orange |
| crystal size (mm) | 0.15 × 0.15 × 0.05 | 0.1 × 0.05 × 0.025 | 0.1 × 0.1 × 0.05 |
| crystal system | monoclinic | orthorhombic | orthorhombic |
| space group | <i>P2₁/m</i> | <i>Cmcm</i> | <i>Pbcn</i> |
| vol (Å ³) | 1146.9(1) | 2334(2) | 1864.1(8) |
| <i>a</i> (Å) | 8.3513(5) | 16.085(7) | 9.434(2) |
| <i>b</i> (Å) | 15.0623(9) | 10.152(4) | 14.676(3) |
| <i>c</i> (Å) | 9.9039(6) | 14.291(6) | 13.464(4) |
| α (deg) | 90 | 90 | 90 |
| β (deg) | 112.981(3) | 90 | 90 |
| γ (deg) | 90 | 90 | 90 |
| <i>Z</i> | 2 | 4 | 4 |
| fw (g/mol) | 660.32 | 691.40 | 609.29 |
| density (calcd) (Mg/m ³) | 1.912 | 1.968 | 2.171 |
| abs coeff (mm ⁻¹) | 7.334 | 7.213 | 9.011 |
| <i>F</i> ₀₀₀ | 622 | 1320 | 1144 |
| total no. reflections | 2451 | 1285 | 1902 |
| unique reflections | 2279 | 1149 | 1177 |
| final <i>R</i> indices [<i>I</i> > 2σ(<i>I</i>)] | <i>R</i> ₁ = 0.0286 <i>wR</i> ₂ = 0.0764 | <i>R</i> ₁ = 0.0360 <i>wR</i> ₂ = 0.0609 | <i>R</i> ₁ = 0.0304 <i>wR</i> ₂ = 0.0510 |
| largest diff peak and hole (e ⁻ Å ⁻³) | 3.015 and -1.765 | 1.386 and -0.822 | 0.896 and -0.971 |
| GOF | 1.107 | 1.052 | 0.949 |
| | 3 | 4 | |
| empirical formula | UF ₆ N ₄ O ₈ S ₂ C ₁₆ H ₁₆ | UF ₆ N ₄ O _{9.5} S ₂ C ₂₄ H ₃₂ | |
| crystal habit, color | block, orange | rod, brown | |
| crystal size (mm) | 0.10 × 0.10 × 0.05 | 0.1 × 0.05 × 0.04 | |
| crystal system | orthorhombic | triclinic | |
| space group | <i>Pna2₁</i> | <i>P</i> $\bar{1}$ | |
| vol (Å ³) | 2378.5(2) | 3159(5) | |
| <i>a</i> (Å) | 11.7508(5) | 12.33(1) | |
| <i>b</i> (Å) | 18.807(1) | 16.38(2) | |
| <i>c</i> (Å) | 10.7623(4) | 16.61(2) | |
| α (deg) | 90 | 90.59(2) | |
| β (deg) | 90 | 100.23(2) | |
| γ (deg) | 90 | 106.38(2) | |
| <i>Z</i> | 4 | 4 | |
| fw (g/mol) | 808.48 | 944.69 | |
| density (calcd) (Mg/m ³) | 2.258 | 1.983 | |
| abs coeff (mm ⁻¹) | 7.098 | 5.363 | |
| <i>F</i> ₀₀₀ | 1528 | 1825 | |
| total no. reflections | 4744 | 10655 | |
| unique reflections | 3857 | 3616 | |
| final <i>R</i> indices [<i>I</i> > 2σ(<i>I</i>)] | <i>R</i> ₁ = 0.0341 <i>wR</i> ₂ = 0.0759 | <i>R</i> ₁ = 0.0612 <i>wR</i> ₂ = 0.0812 | |
| largest diff peak and hole (e ⁻ Å ⁻³) | 1.771 and -2.114 | 1.344 and -1.170 | |
| GOF | 0.930 | 0.823 | |

main residue that exhibit positional disorder. The positional disorder was addressed by modeling the affected atoms in two orientations in a 50:50 ratio. Additionally, complex 2 exhibits some mild positional disorder of the two MeCN solvent molecules. Hydrogen atoms were not assigned to these carbon atoms. Complex 4 exhibits positional disorder of one OTf moiety in the main residue. This disorder was addressed by modeling the OTf moiety in two orientations in a 50:50 ratio. The atoms of the OTf moiety were not refined anisotropically. Complex 4 also contains a THF solvent molecule that exhibited positional disorder, which was addressed by modeling the molecule in two orientations in a 50:50 ratio. Disordered atoms were not refined anisotropically and were constrained with the EADP, DFIX, and FLAT commands. Hydrogen atoms were not assigned to these carbon atoms.

A summary of relevant crystallographic data for 1–4 is presented in Table 3.

[UO₂Cl₂(THF)₂]₂. This complex was prepared according to the published procedure.⁴⁷ Raman (neat solid, cm⁻¹): 1491 (w), 1463 (w), 1460 (w), 1367 (w), 1248 (w), 1231 (w), 1046 (w), 922 (m), 884 (vs), 835 (vs, U=O ν_{sym}), 238 (m), 192 (m), 176 (m).

UO₂(OTf)₂(THF)₃. This complex was prepared according to the published procedure.⁶⁰ Raman (neat solid, cm⁻¹): 1448 (w), 1332 (w), 1233 (m), 1162 (w), 1029 (sh w), 1016 (m), 999 (sh w), 915 (m), 878 (m), 843 (s, U=O ν_{sym}), 758 (m), 580 (w), 564 (w), 346 (w), 343 (w), 317 (m), 177 (m).

UO₂Cl₂(^HN4) (1). To a stirring yellow solution of [UO₂Cl₂(THF)₂]₂ (30.6 mg, 0.032 mmol) in MeCN (2 mL) was added dropwise an off-

white slurry of ${}^{\text{H}}\text{N}_4$ (15.0 mg, 0.062 mmol) in MeCN (1 mL). This resulted in an immediate color change to dark yellow, concomitant with the deposition of yellow solid. The mixture was then allowed to stir at room temperature for 1 h, whereupon the slurry was heated to ca. 70 °C. After 5 min at 70 °C, most of the solid had dissolved, and the yellow-orange slurry was quickly filtered through a diatomaceous earth column (2 cm \times 0.5 cm) supported on glass wool. Storage of the yellow filtrate at -25 °C for 24 h resulted in the deposition of a yellow crystalline solid (24.1 mg, 66% yield). X-ray quality crystals of **1** were grown from a hot, concentrated MeCN solution that was allowed to cool slowly to room temperature. Anal. Calcd for $\text{UCl}_2\text{N}_4\text{O}_2\text{C}_{14}\text{H}_{16}$: C, 28.93; H, 2.77; N, 9.64. Found: C, 29.25; H, 2.42; N, 9.91%. ${}^1\text{H}$ NMR (CD_2Cl_2 , 25 °C, 500 MHz): δ 7.57 (t, $J_{\text{HH}} = 8$ Hz, 2H, aryl CH), 7.17 (d, $J_{\text{HH}} = 8$ Hz, 4H, aryl CH), 5.23 (dd, $J_{\text{HH}} = 6$ Hz, $J_{\text{HH}} = 16$ Hz, 4H, CH_2), 4.82 (d, $J_{\text{HH}} = 16$ Hz, 4H, CH_2). The NH resonance was not observed. ${}^1\text{H}$ NMR (pyr- d_5 , 25 °C, 400 MHz): δ 7.39 (t, $J_{\text{HH}} = 8$ Hz, 2H, aryl CH), 7.05 (d, $J_{\text{HH}} = 8$ Hz, 4H, aryl CH), 6.47 (t, $J_{\text{HH}} = 6$ Hz, 2H, NH), 5.33 (dd, $J_{\text{HH}} = 6$ Hz, $J_{\text{HH}} = 16$ Hz, 4H, CH_2), 4.82 (d, $J_{\text{HH}} = 16$ Hz, 4H, CH_2). IR (KBr pellet, cm^{-1}): 1606 (sh m), 1599 (s), 1583 (m), 1470 (m), 1443 (s), 1423 (sh m), 1379 (m), 1373 (sh w), 1311 (m), 1290 (w), 1255 (w), 1209 (w), 1155 (m), 1088 (m), 1061 (s), 1041 (s), 1010 (sh m), 997 (s), 949 (w), 910 (s), 903 (vs), 889 (vs), 816 (s), 791 (s), 752 (m), 706 (w), 671 (w), 636 (vs), 480 (w). Raman (neat solid, cm^{-1}): 1582 (w), 1395 (w), 1260 (w), 1099 (w), 1015 (m), 910 (w), 813 (vs, $\text{U}=\text{O}$ ν_{sym}), 760 (w), 709 (w), 520 (w), 424 (w), 196 (m).

$\text{UO}_2\text{Cl}_2({}^{\text{Me}}\text{N}_4)$ (**2**). To a stirring yellow solution of $[\text{UO}_2\text{Cl}_2(\text{THF})_2]_2$ (48.5 mg, 0.050 mmol) in MeCN (1 mL) was added dropwise a colorless solution of ${}^{\text{Me}}\text{N}_4$ (24.3 mg, 0.091 mmol) in MeCN (1 mL). This resulted in an immediate color change to orange-yellow, concomitant with the deposition of an orange-yellow precipitate. This orange-yellow slurry was allowed to stir at room temperature for 10 min, whereupon the orange-yellow solid was isolated by decanting the supernatant. The solid was washed with Et_2O (1 mL) and then dried in vacuo (41.8 mg, 73% yield). X-ray quality crystals of **2** were grown from a concentrated MeCN solution layered with an equal volume of Et_2O , which was stored at -25 °C for 24 h. Anal. Calcd for $\text{UCl}_2\text{N}_4\text{O}_2\text{C}_{16}\text{H}_{20}$: C, 31.54; H, 3.31; N, 9.20. Found: C, 31.17; H, 2.58; N, 10.35%. ${}^1\text{H}$ NMR (CD_2Cl_2 , 25 °C, 400 MHz): δ 7.52 (t, $J_{\text{HH}} = 8$ Hz, 2H, aryl CH), 7.05 (d, $J_{\text{HH}} = 8$ Hz, 4H, aryl CH), 4.85 (d, $J_{\text{HH}} = 15$ Hz, 4H, CH_2), 4.29 (d, $J_{\text{HH}} = 15$ Hz, 4H, CH_2), 3.57 (s, 6H, CH_3). IR (KBr pellet, cm^{-1}): 1597 (m), 1578 (w), 1468 (m), 1452 (sh m), 1446 (s), 1427 (sh w), 1385 (m), 1367 (w), 1309 (w), 1263 (w), 1254 (w), 1232 (w), 1219 (m), 1182 (w), 1165 (m), 1093 (sh w), 1088 (m), 1082 (m), 1014 (s), 980 (w), 951 (w), 895 (vs), 885 (sh m), 812 (sh w), 802 (s), 762 (m), 727 (w), 636 (w), 538 (w), 471 (w), 455 (w). Raman (neat solid, cm^{-1}): 1580 (w), 1465 (w), 1454 (w), 1386 (w), 1258 (w), 1085 (w), 1015 (m), 815 (s, $\text{U}=\text{O}$ ν_{sym}), 769 (w), 730 (w), 403 (m), 396 (m), 284 (m), 240 (m), 199 (m), 152 (m), 118 (vs).

$\text{UO}_2(\text{OTf})_2({}^{\text{H}}\text{N}_4)$ (**3**). To a stirring yellow solution of $\text{UO}_2(\text{OTf})_2(\text{THF})_3$ (49.5 mg, 0.063 mmol) in MeCN (1 mL) was added dropwise an off-white slurry of ${}^{\text{H}}\text{N}_4$ (14.6 mg, 0.061 mmol) in MeCN (1 mL). This resulted in an immediate color change to orange. The orange solution was allowed to stir at room temperature for 10 min, whereupon it was filtered through a diatomaceous earth column (2 cm \times 0.5 cm) supported on glass wool. The resulting orange filtrate was concentrated in vacuo to ca. 1 mL and layered with Et_2O (3 mL). Storage of this solution at -25 °C for 24 h resulted in the deposition of orange powder (38.6 mg, 76% yield). X-ray quality crystals were grown from a MeCN solution layered with an equal volume of Et_2O , which was stored at -25 °C for 24 h. Anal. Calcd for $\text{UF}_6\text{N}_4\text{O}_8\text{S}_2\text{C}_{16}\text{H}_{16}$: C, 23.77; H, 1.99; N, 6.93. Found: C, 24.19; H, 1.21; N, 7.09%. ${}^1\text{H}$ NMR (CD_2Cl_2 , 25 °C, 400 MHz): δ 7.66 (t, $J_{\text{HH}} = 8$ Hz, 2H, aryl CH), 7.29 (d, $J_{\text{HH}} = 8$ Hz, 4H, aryl CH), 5.76 (br s, 2H, NH), 5.19 (dd, $J_{\text{HH}} = 5$ Hz, $J_{\text{HH}} = 16$ Hz, 4H, CH_2), 4.91 (d, $J_{\text{HH}} = 16$ Hz, 4H, CH_2). ${}^1\text{H}$ NMR (pyr- d_5 , 25 °C, 400 MHz): δ 7.59 (br t, $J_{\text{HH}} = 9$ Hz, 2H, aryl CH), 7.28 (d, $J_{\text{HH}} = 7$ Hz, 4H, aryl CH), 6.17 (br s, 2H, NH), 5.23 (br d, $J_{\text{HH}} = 14$ Hz, 4H, CH_2), 4.96 (d, $J_{\text{HH}} = 16$ Hz, 4H, CH_2). ${}^{19}\text{F}\{^1\text{H}\}$ NMR (CD_2Cl_2 , 25 °C, 376 MHz): δ -77.41 . ${}^{19}\text{F}\{^1\text{H}\}$

NMR (pyr- d_5 , 25 °C, 376 MHz): δ -77.29 . IR (KBr pellet, cm^{-1}): 1610 (sh w), 1603 (w), 1585 (w), 1475 (w), 1450 (m), 1325 (s), 1309 (sh m), 1296 (m), 1252 (sh m), 1232 (s), 1203 (s), 1198 (s), 1178 (s), 1171 (sh m), 1088 (w), 1068 (w), 1057 (m), 1026 (m), 1009 (vs), 950 (w), 942 (sh w), 903 (s), 825 (w), 802 (m), 796 (w), 756 (w), 633 (vs), 579 (w), 571 (w), 515 (m). Raman (neat solid, cm^{-1}): 1587 (w), 1474 (w), 1393 (w), 1264 (w), 1243 (w), 1079 (w), 1028 (m), 833 (s, $\text{U}=\text{O}$ ν_{sym}), 762 (m), 585 (w), 574 (w), 415 (m), 349 (w), 325 (w), 181 (w).

$[\text{UO}_2(\text{OTf})(\text{THF})({}^{\text{Me}}\text{N}_4)](\text{OTf})$ (**4**). To a stirring yellow solution of $\text{UO}_2(\text{OTf})_2(\text{THF})_3$ (67.1 mg, 0.086 mmol) in THF (1.5 mL) was added dropwise a colorless solution of ${}^{\text{Me}}\text{N}_4$ (22.0 mg, 0.082 mmol) in THF (1 mL). This resulted in the immediate color change to orange. The mixture was allowed to stir at room temperature for 10 min, whereupon it was filtered through a diatomaceous earth column (2 cm \times 0.5 cm) supported on glass wool. The resulting orange filtrate was then layered with Et_2O (1 mL). Storage of this solution at -25 °C for 24 h resulted in the deposition of an orange powder, which was isolated by decanting the supernatant (56.8 mg, 73% yield). X-ray quality crystals were grown in a two-vial system, whereby a THF solution (3 mL) of **4** was transferred to a 4 mL scintillation vial that was placed inside a 20 mL scintillation vial. Et_2O (2 mL) was then added to the outer vial. Storage of this two-vial system at -25 °C for 24 h afforded orange X-ray quality crystals. Anal. Calcd for $\text{UF}_6\text{N}_4\text{O}_8\text{S}_2\text{C}_{22}\text{H}_{28}$: C, 29.08; H, 3.11; N, 6.17. Found: C, 29.50; H, 3.07; N, 5.89%. ${}^1\text{H}$ NMR (CD_2Cl_2 , 25 °C, 400 MHz): δ 7.67 (t, $J_{\text{HH}} = 8$ Hz, 2H, aryl CH), 7.23 (d, $J_{\text{HH}} = 8$ Hz, 4H, aryl CH), 4.87 (d, $J_{\text{HH}} = 15$ Hz, 4H, CH_2), 4.53 (d, $J_{\text{HH}} = 15$ Hz, 4H, CH_2), 3.73 (br s, 4H, THF), 3.59 (br s, 6H, CH_3), 1.84 (br s, 4H, THF). ${}^1\text{H}$ NMR (pyr- d_5 , 25 °C, 400 MHz): δ 7.59 (br s, 2H, aryl CH), 7.22 (br s, 4H, aryl CH), 4.94 (d, $J_{\text{HH}} = 15$ Hz, 4H, CH_2), 4.78 (d, $J_{\text{HH}} = 16$ Hz, 4H, CH_2), 3.66 (br s, 4H, THF), 2.93 (br s, 6H, CH_3), 1.62 (br s, 4H, THF). ${}^{19}\text{F}\{^1\text{H}\}$ NMR (CD_2Cl_2 , 25 °C, 376 MHz): δ -77.57 . ${}^{19}\text{F}\{^1\text{H}\}$ NMR (pyr- d_5 , 25 °C, 376 MHz): δ -77.41 . IR (KBr pellet, cm^{-1}): 3049 (w), 3006 (sh w), 2980 (m), 2962 (sh m), 2943 (sh m), 2877 (w), 2873 (w), 2806 (sh vw), 1603 (m), 1583 (m), 1470 (sh m), 1462 (m), 1452 (sh m), 1390 (w), 1362 (sh w), 1327 (s), 1265 (s), 1255 (s), 1234 (s), 1223 (m), 1205 (s), 1173 (sh m), 1155 (s), 1080 (sh w), 1068 (w), 1065 (w), 1030 (s), 1012 (s), 957 (w), 912 (m), 883 (m), 866 (m), 854 (m), 812 (m), 768 (m), 756 (w), 729 (w), 636 (vs), 580 (sh w), 573 (m), 526 (w), 517 (m), 471 (w). Raman (neat solid, cm^{-1}): 1608 (w), 1585 (w), 1465 (w), 1391 (w), 1262 (m), 1237 (w), 1227 (w), 1079 (w), 1030 (m), 1028 (m), 924 (w), 831 (s, $\text{U}=\text{O}$ ν_{sym}), 766 (w), 764 (w), 574 (w), 418 (m), 347 (w), 187 (w), 116 (m).

■ ASSOCIATED CONTENT

Supporting Information

The Supporting Information is available free of charge on the ACS Publications website at DOI: 10.1021/acs.inorgchem.6b00799.

Crystallographic details for compounds **1**–**4**. (CIF)

Spectral data for compounds **1**–**4**. (PDF)

■ AUTHOR INFORMATION

Corresponding Author

*E-mail: hayton@chem.ucsb.edu.

Notes

The authors declare no competing financial interest.

■ ACKNOWLEDGMENTS

This work was supported by the U.S. Department of Energy, Office of Basic Energy Sciences, Chemical Sciences, Biosciences, and Geosciences Division under Contract No. DE-SC-0001861 (to T.W.H.) and Contract No. DE-FG02-11ER16254 (to L.M.M.).

REFERENCES

- (1) Denning, R. G. *J. Phys. Chem. A* **2007**, *111*, 4125–4143.
- (2) Cotton, S. *Lanthanide and Actinide Chemistry*; John Wiley & Sons, Ltd: West Sussex, England, 2006.
- (3) Duval, P. B.; Burns, C. J.; Buschmann, W. E.; Clark, D. L.; Morris, D. E.; Scott, B. L. *Inorg. Chem.* **2001**, *40*, 5491–5496.
- (4) Arney, D. S. J.; Burns, C. J. *J. Am. Chem. Soc.* **1995**, *117*, 9448–9460.
- (5) Villiers, C.; Thuéry, P.; Ephritikhine, M. *Angew. Chem., Int. Ed.* **2008**, *47*, 5892–5893.
- (6) Vaughn, A. E.; Barnes, C. L.; Duval, P. B. *Angew. Chem., Int. Ed.* **2007**, *46*, 6622–6625.
- (7) Cantat, T.; Graves, C. R.; Scott, B. L.; Kiplinger, J. L. *Angew. Chem., Int. Ed.* **2009**, *48*, 3681–3684.
- (8) Duval, P. B.; Burns, C. J.; Clark, D. L.; Morris, D. E.; Scott, B. L.; Thompson, J. D.; Werkema, E. L.; Jia, L.; Andersen, R. A. *Angew. Chem., Int. Ed.* **2001**, *40*, 3357–3361.
- (9) Arney, D. S. J.; Burns, C. J.; Smith, D. C. *J. Am. Chem. Soc.* **1992**, *114*, 10068–10069.
- (10) Spencer, L. P.; Gdula, R. L.; Hayton, T. W.; Scott, B. L.; Boncella, J. M. *Chem. Commun.* **2008**, 4986–4988.
- (11) Hayton, T. W.; Boncella, J. M.; Scott, B. L.; Batista, E. R.; Hay, P. J. *J. Am. Chem. Soc.* **2006**, *128*, 10549–10559.
- (12) Arnold, P. L.; Jones, G. M.; Odoh, S. O.; Schreckenbach, G.; Magnani, N.; Love, J. B. *Nat. Chem.* **2012**, *4*, 221–227.
- (13) Jones, G. M.; Arnold, P. L.; Love, J. B. *Angew. Chem., Int. Ed.* **2012**, *51*, 12584–12587.
- (14) Schreckenbach, G.; Hay, P. J.; Martin, R. L. *Inorg. Chem.* **1998**, *37*, 4442–4451.
- (15) Bühl, M.; Schreckenbach, G. *Inorg. Chem.* **2010**, *49*, 3821–3827.
- (16) Mullane, K. C.; Lewis, A. J.; Yin, H.; Carroll, P. J.; Schelter, E. J. *Inorg. Chem.* **2014**, *53*, 9129–9139.
- (17) La Pierre, H. S.; Meyer, K. *Inorg. Chem.* **2013**, *52*, 529–539.
- (18) Kovács, A.; Konings, R. J. M. *ChemPhysChem* **2006**, *7*, 455–462.
- (19) Lam, O. P.; Franke, S. M.; Nakai, H.; Heinemann, F. W.; Hieringer, W.; Meyer, K. *Inorg. Chem.* **2012**, *51*, 6190–6199.
- (20) Lewis, A. J.; Carroll, P. J.; Schelter, E. J. *J. Am. Chem. Soc.* **2013**, *135*, 511–518.
- (21) Pedrick, E. A.; Wu, G.; Kaltsoyannis, N.; Hayton, T. W. *Chem. Sci.* **2014**, *5*, 3204–3213.
- (22) Burrell, A. K.; Hemmi, G.; Lynch, V.; Sessler, J. L. *J. Am. Chem. Soc.* **1991**, *113*, 4690–4692.
- (23) Sessler, J. L.; Vivian, A. E.; Seidel, D.; Burrell, A. K.; Hoehner, M.; Mody, T. D.; Gebauer, A.; Weghorn, S. J.; Lynch, V. *Coord. Chem. Rev.* **2001**, *216–217*, 411–434.
- (24) Liao, M.-S.; Kar, T.; Scheiner, S. *J. Phys. Chem. A* **2004**, *108*, 3056–3063.
- (25) Khusnutdinova, J. R.; Luo, J.; Rath, N. P.; Mirica, L. M. *Inorg. Chem.* **2013**, *52*, 3920–3932.
- (26) Khusnutdinova, J. R.; Rath, N. P.; Mirica, L. M. *Inorg. Chem.* **2014**, *53*, 13112–13129.
- (27) Zheng, B.; Tang, F.; Luo, J.; Schultz, J. W.; Rath, N. P.; Mirica, L. M. *J. Am. Chem. Soc.* **2014**, *136*, 6499–6504.
- (28) Kiernicki, J. J.; Cladis, D. P.; Fanwick, P. E.; Zeller, M.; Bart, S. C. *J. Am. Chem. Soc.* **2015**, *137*, 11115–11125.
- (29) Maynadie, J.; Berthet, J.-C.; Thuery, P.; Ephritikhine, M. *Chem. Commun.* **2007**, 486–488.
- (30) Tourneux, J.-C.; Berthet, J.-C.; Cantat, T.; Thuery, P.; Mezaillies, N.; Ephritikhine, M. *J. Am. Chem. Soc.* **2011**, *133*, 6162–6165.
- (31) Lu, E.; Cooper, O. J.; McMaster, J.; Tuna, F.; McInnes, E. J. L.; Lewis, W.; Blake, A. J.; Liddle, S. T. *Angew. Chem., Int. Ed.* **2014**, *53*, 6696–6700.
- (32) Wilkerson, M. P.; Burns, C. J.; Morris, D. E.; Paine, R. T.; Scott, B. L. *Inorg. Chem.* **2002**, *41*, 3110–3120.
- (33) Berthet, J.-C.; Thuéry, P.; Dognon, J.-P.; Guillaneux, D.; Ephritikhine, M. *Inorg. Chem.* **2008**, *47*, 6850–6862.
- (34) Raffard, N.; Carina, R.; Simaan, A. J.; Sinton, J.; Rivière, E.; Tchertanov, L.; Bourcier, S.; Bouchoux, G.; Delroisse, M.; Banse, F.; Girerd, J.-J. *Eur. J. Inorg. Chem.* **2001**, *2001*, 2249–2254.
- (35) Chow, T. W.-S.; Wong, E. L.-M.; Guo, Z.; Liu, Y.; Huang, J.-S.; Che, C.-M. *J. Am. Chem. Soc.* **2010**, *132*, 13229–13239.
- (36) Koch, W. O.; Kaiser, J. T. *Chem. Commun.* **1997**, 2237–2238.
- (37) Koch, W. O.; Barbieri, A.; Grodzicki, M.; Schünemann, V.; Trautwein, A. X.; Krüger, H.-J. *Angew. Chem., Int. Ed. Engl.* **1996**, *35*, 422–424.
- (38) Lee, W.-T.; Muñoz, S. B.; Dickie, D. A.; Smith, J. M. *Angew. Chem., Int. Ed.* **2014**, *53*, 9856–9859.
- (39) Sugimoto, H.; Ashikari, K.; Itoh, S. *Inorg. Chem.* **2013**, *52*, 543–545.
- (40) Albela, B.; Carina, R.; Polcar, C.; Poussereau, S.; Cano, J.; Guilhem, J.; Tchertanov, L.; Blondin, G.; Delroisse, M.; Girerd, J.-J. *Inorg. Chem.* **2005**, *44*, 6959–6966.
- (41) Copping, R.; Jeon, B.; Pemmaraju, C. D.; Wang, S.; Teat, S. J.; Janousch, M.; Tyliczszak, T.; Canning, A.; Grønbech-Jensen, N.; Prendergast, D.; Shuh, D. K. *Inorg. Chem.* **2014**, *53*, 2506–2515.
- (42) Schettini, M. F.; Wu, G.; Hayton, T. W. *Inorg. Chem.* **2009**, *48*, 11799–11808.
- (43) Berthet, J.-C.; Nierlich, M.; Ephritikhine, M. *Dalton Trans.* **2004**, 2814–2821.
- (44) Sarsfield, M. J.; Steele, H.; Helliwell, M.; Teat, S. J. *Dalton Trans.* **2003**, 3443–3449.
- (45) Sarsfield, M. J.; Helliwell, M.; Collison, D. *Chem. Commun.* **2002**, 2264–2265.
- (46) Berthet, J.-C.; Nierlich, M.; Ephritikhine, M. *Chem. Commun.* **2003**, 1660–1661.
- (47) Wilkerson, M. P.; Burns, C. J.; Paine, R. T.; Scott, B. L. *Inorg. Chem.* **1999**, *38*, 4156–4158.
- (48) Fortier, S.; Hayton, T. W. *Coord. Chem. Rev.* **2010**, *254*, 197–214.
- (49) Nguyen Trung, C.; Begun, G. M.; Palmer, D. A. *Inorg. Chem.* **1992**, *31*, 5280–5287.
- (50) Brown, J. L.; Mokhtarzadeh, C. C.; Lever, J. M.; Wu, G.; Hayton, T. W. *Inorg. Chem.* **2011**, *50*, 5105–5112.
- (51) Clark, D. L.; Conradson, S. D.; Donohoe, R. J.; Keogh, D. W.; Morris, D. E.; Palmer, P. D.; Rogers, R. D.; Tait, C. D. *Inorg. Chem.* **1999**, *38*, 1456–1466.
- (52) Pedrick, E. A.; Wu, G.; Hayton, T. W. *Inorg. Chem.* **2015**, *54*, 7038–7044.
- (53) Cornet, S. M.; May, I.; Redmond, M. P.; Selvage, A. J.; Sharrad, C. A.; Rosnel, O. *Polyhedron* **2009**, *28*, 363–369.
- (54) Khusnutdinova, J. R.; Rath, N. P.; Mirica, L. M. *J. Am. Chem. Soc.* **2010**, *132*, 7303–7305.
- (55) Tang, F.; Zhang, Y.; Rath, N. P.; Mirica, L. M. *Organometallics* **2012**, *31*, 6690–6696.
- (56) Tang, F.; Qu, F.; Khusnutdinova, J. R.; Rath, N. P.; Mirica, L. M. *Dalton Trans.* **2012**, *41*, 14046–14050.
- (57) Berthet, J.-C.; Siffredi, G.; Thuery, P.; Ephritikhine, M. *Dalton Trans.* **2009**, 3478–3494.
- (58) Weisman, G. R.; Wong, E. H.; Hill, D. C.; Rogers, M. E.; Reed, D. P.; Calabrese, J. C. *Chem. Commun.* **1996**, 947–948.
- (59) Wong, E. H.; Weisman, G. R.; Hill, D. C.; Reed, D. P.; Rogers, M. E.; Condon, J. S.; Fagan, M. A.; Calabrese, J. C.; Lam, K.-C.; Guzei, I. A.; Rheingold, A. L. *J. Am. Chem. Soc.* **2000**, *122*, 10561–10572.
- (60) Oldham, S. M.; Scott, B. L.; Oldham, W. J. *Appl. Organomet. Chem.* **2006**, *20*, 39–43.
- (61) Alpha, B.; Anklam, E.; Deschenaux, R.; Lehn, J.-M.; Pietraskiewicz, M. *Helv. Chim. Acta* **1988**, *71*, 1042–1052.
- (62) Bottino, F.; Di Grazia, M.; Finocchiaro, P.; Fronczek, F. R.; Mamo, A.; Pappalardo, S. *J. Org. Chem.* **1988**, *53*, 3521–3529.
- (63) Harris, R. K.; Becker, E. D.; Cabral De Menezes, S. M.; Goodfellow, R.; Granger, P. *Pure Appl. Chem.* **2001**, *73*, 1795–1818.
- (64) Harris, R. K.; Becker, E. D.; Cabral De Menezes, S. M.; Granger, P.; Hoffman, R. E.; Zilm, K. W. *Pure Appl. Chem.* **2008**, *80*, 59–84.
- (65) SMART, Apex II, Version 2.1; Bruker AXS Inc: Madison, WI, 2005.
- (66) SAINT, Software User's Guide, Version 7.34a; Bruker AXS Inc: Madison, WI, 2005.

(67) Sheldrick, G. M. *SADABS*, University of Gottingen: Germany, 2005.

(68) *SHELXTL PC*, Version 6.12; Bruker AXS Inc: Madison, WI, 2005.

(69) Sheldrick, G. M. *CELL_NOW*, Version 2008–4; Bruker AXS Inc: Madison, WI, 2008.